Anisotropic Goal-oriented estimate for a third-order accurate Euler model

A. Carabias[b], A. Belme[b], F. Alauzet[a], A. Loseille[a], A. Dervieux[b]

[a] *INRIA, Projet Gamma, Domaine de Voluceau, Rocquencourt, BP 105, 78153 Le Chesnay Cedex, France.*
[b] *INRIA, Projet Tropics, 2004 route des lucioles - BP 93, 06902 Sophia Antipolis Cedex, France*

Abstract

Initially restricted to interpolation errors, *a priori* anisotropic goal-oriented error estimates have become an efficient tool for addressing steady Euler flows [10], unsteady Euler flows [5],[6], and more recently steady and unsteady Navier-Stokes ones [4]. Estimates are obtained for a second-order mixed-element-volume approximation close to the usual P^1 finite element. Promises given by theory were kept by numerical demonstrators, showing second-order convergence for shocked flows. The theory also predicts higher-order convergence for the higher-order interpolation of singular flows. For this, higher-order anisotropic estimates are needed. In this paper we consider a central-ENO approximation for the Euler equations. The scheme is third-order accurate on irregular unstructured meshes. The implicit error method is extended to this new context. The resulting *a priori* error analysis is a kind of dual of the *a posteriori* analysis of Barth and Larson [3]. We exploit the principal direction representation of Cao [7]. Then an optimum problem for the mesh metric is obtained and analytically solved. The resulting mesh optimality system is discretised and solved thanks to the global unsteady fixed point algorithm of [5]. The new method is applied to an acoustic propagation benchmark and compared with previous approaches.

Key words: Computational Fluid Dynamics, high order approximation, mesh adaptation

1. Introduction

Initially restricted to interpolation errors, *a priori* anisotropic error estimates are available for goal-oriented formulations, and have become an efficient tool for addressing steady Euler flows [10], unsteady Euler flows [5], and more recently steady and unsteady Navier-Stokes ones [4]. The error analysis followed the so-called implicit error method, dealing with a discrete invertible system for the deviation between discrete solution and a projection of the continuous one. Estimates were

obtained for a second-order mixed-element-volume approximation close to the usual $\mathcal{P}^1$ finite element. Promises given by theory were kept by numerical demonstrators, showing second convergence for shocked flows. The theory also predicts higher-order convergence for the higher-order interpolation of singular flows. For their approximation by a higher-order scheme, anisotropic estimates are needed.

In this paper we consider a central-ENO approximation for the Euler equations. The scheme is third-order accurate on irregular unstructured meshes. The implicit error method is extended to this new context. The resulting *a priori* error analysis is a kind of dual of the *a posteriori* analysis of Barth and Larson [3]. We exploit the principal direction representation of Cao [7]. Then an optimisation problem for the mesh metric is obtained and analytically solved. For solving the resulting mesh optimality system, we discretise it and apply the global unsteady fixed point algorithm of [5, 6].

The new method is applied to an acoustic propagation benchmark and compared with previous approaches.

2. Numerical approximation

2.1. Model

The 2D Euler equations in a geometrical domain Ω of boundary Γ can be written:

$$\text{Find } u \in \mathcal{V} \text{ such that } \int_\Omega v \nabla \cdot \mathcal{F}(u)\ d\ \Omega = \int_\Gamma v \mathcal{F}_\Gamma(u)\ d\ \Gamma\ \forall\ v \in \mathcal{V}. \tag{1}$$

Here $u = (u_1, u_2, u_3, u_4)$ holds for the conserved unknowns (density, moments components, energy) and $\mathcal{F}$ for the usual Euler fluxes. As right-hand side we have an integral of the various boundary fluxes $\mathcal{F}_\Gamma$ for various boundary conditions, which we do not need to detail here. Defining

$$B(u, v) = \int_\Omega v \nabla \cdot \mathcal{F}(u)\ d\ \Omega$$

and

$$F_u(v) = \int_\Gamma v \mathcal{F}_\Gamma(u)\ d\ \Gamma,$$

this writes:

$$\text{Find } u \in \mathcal{V} \text{ such that } B(u, v) = F_u(v)\ \forall\ v \in \mathcal{V}. \tag{2}$$

2.2. CENO formulation

We choose a reconstruction-based finite-volume method, getting inspired by the unlimited version of the reconstruction technique of Barth [2] and of Central-ENO (CENO) methods developed by

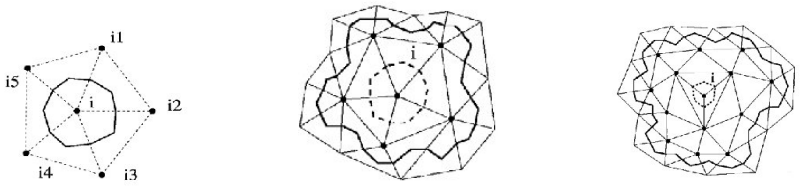

Figure 1: Dual cell and two reconstruction molecules

Groth and co-workers, [9]. Concerning the location of nodes with respect to mesh elements, we prefer to minimize the number of unknowns with respect to a given mesh and therefore we keep the vertex-centered location already successfully used for second-order anisotropic (Hessian-based or Goal-oriented) mesh adaptation. The considered numerical approximation is described in details in [8]. Its main features are: (a) vertex centered, (b) dual median cells around the vertex, (c) a single mean square conservative quadratic reconstruction for each dual cell (d) HLLC Riemann solver for fluxes integration, (e) explicit multi-stage time-stepping.

The computational domain is divided in triangles and in a dual tesselation in cells, each cell C_i being built around a vertex i, with limits following sections of triangle medians.

We define the discrete space $\mathcal{V}_0$ of functions that are constant on any dual cell C_i.

Let us define a reconstruction operator R_2^0 which reconstructs a function of $\mathcal{V}_0$ in each cell C_i under the form of a second-order polynomial:

$$R_2^0 u_0|_{C_i} = \mathcal{P}_i(X).$$

Given the means $(\overline{u_{0,i}}, i = 1, ...)$ of u_0 on cells i of centroid G_i, find the $c_{i,\alpha}$, $|\alpha| \leq k$ such that

$$\overline{\mathcal{P}_{i,i}} = \overline{u_{0,i}} \qquad \sum_{j \in N(i)} (\overline{\mathcal{P}_{i,j}} - \overline{u_{0,j}})^2 = Min$$

with

$$\mathcal{P}_i(x) = \overline{u_{0,i}} + \sum_{|\alpha| \leq k} c_{i,\alpha}[(X - G_i)^\alpha - \overline{(X - G_i)^\alpha}]$$

and where $\overline{\mathcal{P}_{i,j}}$ stands for the mean of $\mathcal{P}_i(X)$ on cell j.

For the Euler model (2), the discrete CENO version writes:

$$\text{Find } u_0 \in \mathcal{V}_0 \text{ such that } B(R_2^0 u_0, v_0) = F_{R_2^0 u_0}(v_0) \ \forall \ v_0 \in \mathcal{V}_0$$

We observe that this produces a finite volume formulation:

$$\forall C_i, \quad \int \nabla \cdot \mathcal{F}(R_2^0 u_0) \ d\ \Omega = \int_{\partial C_i \cap \Gamma} \mathcal{F}_\Gamma(R_2^0 u_0) \ d\ \Gamma$$

or:

$$\forall C_i, \quad \int_{\partial C_i} \mathcal{F}(R_2^0 u_0) \cdot \mathbf{n} \; d\,\Gamma - \int_{\partial C_i \cap \Gamma} \mathcal{F}_\Gamma(R_2^0 u_0) \; d\,\Gamma = 0. \tag{3}$$

The knowledge of the reconstruction does not completely define the CENO approximation. Indeed, the reconstruction performed in each cell is generally discontinuous at cell interfaces. In order to fix an integration value at the interface, we can consider an arithmetic mean of the fluxes values for the two reconstruction values:

$$\mathcal{F}(R_2^0 u_0)^{quadrature}|_{\partial C_i \cap \partial C_j} \cdot \mathbf{n} = \frac{1}{2}\left(\mathcal{F}(R_2^0 u_0)|_{\partial C_i} + \mathcal{F}(R_2^0 u_0)|_{\partial C_j}\right) \cdot \mathbf{n} \tag{4}$$

where $(R_2^0 u_0)|_{\partial C_i}$ holds for the value at cell boundary of the reconstructed $R_2^0 u_0|_{C_i}$ on cell C_i. The above mean is applied on Gauss integration points (two per interface segment). This formulation produces a central-differenced numerical approximation which is third order accurate, but it cannot be used as it is in nonlinear applications, due to a lack of stability.

2.3. Vertex-centered low dissipation CENO2

Scheme (3) is usually combined with an approximate Riemann solver used instead of (4). This latter option produces a rather dissipative third-order accurate scheme. Now we are here interested only by rather mild non-linear effects. Scheme (3)(4) is instead stabilized as in [1], *i.e* completed by two extra terms: the first term compensate partially the main dispersive error. The second one introduces a sixth order dissipation. We refer to [1] for details and for numerical experiments showing the interest of this new CENO2 variant.

3. Error analysis

We drive an *a priori* analysis which is in some manner the dual of the *a posteriori* analysis proposed in [3]. Let be $j(u) = (g, u)$ the scalar output which we want to accurately compute. We concentrate the reduction by mesh adaption of the following error:

$$\delta j = (g, R_2^0 \pi_0 u - R_2^0 u_0)$$

where g is function of $L^2(\Omega)$. The adjoint state $u_0^* \in \mathcal{V}_0$ is the solution of:

$$\frac{\partial B}{\partial u}(R_2^0 u_0)(R_2^0 v_0, u_0^*) = (g, R_2^0 v_0), \; \forall \; v_0 \in \mathcal{V}_0.$$

We also need to define the projection π_0:

$$\begin{aligned} \pi_0 : (V) &\to (V_0), \\ v &\mapsto \pi_0 v \\ \forall\ C_i, \text{dual cell}, \pi_0 v|_{C_i} &= \int_{C_i} v dx. \end{aligned}$$

Then we can write, successively:

$$\begin{aligned} (g, R_2^0\pi_0 u - R_2^0 u_0) &= \tfrac{\partial B}{\partial u}(R_2^0 u_0)(R_2^0\pi_0 u - R_2^0 u_0, u_0^*) \quad \text{(adjoint eq.)} \\ &\approx B(R_2^0\pi_0 u, u_0^*) - B(R_2^0 u_0, u_0^*) \end{aligned}$$

and then

$$\begin{aligned} &(g, R_2^0\pi_0 u - R_2^0 u_0) \\ &\qquad \approx \quad B(R_2^0\pi_0 u, u_0^*) - F_{R_2^0 u_0}(u_0^*) \qquad \text{(disc.state eq.)} \\ &\qquad \approx \quad B(R_2^0\pi_0 u, u_0^*) - B(u, u_0^*) - F_{R_2^0 u_0}(u_0^*) + F_u(u_0^*) \qquad \text{(cont.state eq.)} \\ &\qquad \approx \quad \tfrac{\partial B}{\partial u}(u)(R_2^0\pi_0 u - u, u_0^*) - \tfrac{\partial F}{\partial u}(u).(R_2^0\pi_0 u - u).(u_0^*) \end{aligned}$$

In this study, we do not consider the adaptation of boundary mesh and as in [10] we discard the boundary terms. Then the case of Euler equations is written:

$$\frac{\partial B}{\partial u}(u)(R_2^0\pi_0 u - u, u_0^*) \approx \sum_i \int_{C_i} u_0^* \nabla \cdot \mathcal{F}'(u)(R_2^0\pi_0 u - u) dx$$

where the sum applies for all dual cell C_i of the mesh. Noting that u_0 is constant over each cell C_i, we can transform the above with an integration by parts (again terms on $\partial\Omega$ are skipped):

$$\frac{\partial B}{\partial u}(u)(R_2^0\pi_0 u - u, u_0^*) \approx -\sum_i \int_{\partial C_i} u_0^* \mathcal{F}'(R_2^0\pi_0 u - u) \cdot \mathbf{n}\ \mathrm{d}\sigma.$$

Observing that two integrals are computed on each interface C_{ij} separating two neighboring cells:

$$\frac{\partial B}{\partial u}(u)(R_2^0\pi_0 u - u, u_0^*) \approx -\sum_{C_{ij}} \int_{\partial C_i \cap \partial C_j} \left[\left(u_0^* \mathcal{F}'(R_2^0\pi_0 u - u)\right)_{C_i} - \left(u_0^* \mathcal{F}'(R_2^0\pi_0 u - u)\right)_{C_j} \right] \cdot \mathbf{n}\ \mathrm{d}\sigma.$$

Even for $u_0^* \approx \pi_0 u^*$, with u^* smooth, the discontinuity at interface of u_0^* is of order 1. By construction of the higher order reconstruction, the discontinuity at interface of $R_2^0\pi_0 u - u$ is of higher order and can be neglected. Then:

$$\begin{aligned} &\left(u_0^* \mathcal{F}'(R_2^0\pi_0 u - u)\right)_{C_i} - \left(u_0^* \mathcal{F}'(R_2^0\pi_0 u - u)\right)_{C_j} \approx \\ &\qquad \frac{1}{2}\left[(u_0^*)_{C_i} - (u_0^*)_{C_j}\right] \left[\left(\mathcal{F}'(R_2^0\pi_0 u - u)\right)_{C_i} + \left(\mathcal{F}'(R_2^0\pi_0 u - u)\right)_{C_j} \right] \end{aligned}$$

We shall show that $R_2^0\pi_0 u - u$ can be replaced by a smooth function of the local third derivatives and local mesh size:

$$R_2^0\pi_0 u_q - u_q \approx G(u_q^{(3)}, (\delta\mathbf{x})^3), \quad \forall\ q = 1, 4,$$

and for each flux component ($r = 1, 2$)

$$\mathcal{F}'_r(R_2^0\pi_0 u - u) \approx \sum_q\ \mathcal{F}'_{qr}(G(u_q^{(3)}, (\delta\mathbf{x})^3)).$$

On the other side, the jump term $u_0^*|_{C_i} - u_0^*|_{C_j}$ is a first derivative of u^* times the distance between the centroids of the two cells, or equivalently (at first-order) the vertices i and j. The integration of this term over the section of interface $\partial C_i \cap \partial C_j$ is essentially the (double of the) area of the four triangles delimited by i, j and the centroids of triangles havin ij as common side. The set of all these triangles is a tessellation of the computationa domain. Then:

$$|\delta j| \approx |\frac{\partial B}{\partial u}(u)(R_2^0\pi_0 u - u, u_0^*)| \approx 2\sum_q \int_\Omega K_q(u, u^*)|G(u_q^{(3)}, (\delta\mathbf{x})^3)|\ \mathrm{d}\Omega$$

with

$$K_q(u, u^*) = \sum_r |(\mathcal{F}'_{rq}(u))^*||\frac{\partial u_q^*}{\partial x_r}|.$$

The error is expressed in terms of the $\delta\mathbf{x}$), measuring local mesh size. We consider now a way to find the mesh which minimizes this error.

Optimal metric

The parametrization of the mesh is a Riemannian metric defined in each point $\mathbf{x} = (x, y)$ of the computational domain by a symmetric matrix,

$$\mathcal{M}(\mathbf{x}) = d\ \mathcal{R}(\mathbf{x})\Lambda(\mathbf{x})\mathcal{R}^t(\mathbf{x}).$$

The rotation matrix $\mathcal{R} = (\mathbf{e}_\xi, \mathbf{e}_\eta)$, built with the normalised eigenvectors $\mathbf{e}_\xi = (e_\xi^x, e_\xi^y)$ and $\mathbf{e}_\eta = (e_\eta^x, e_\eta^y)$ of $\mathcal{M}$, parametrizes the two orthogonal stretching directions of the metric. Denoting m_ξ and m_η the two directional local mesh sizes in the characteristic/stretching directions of $\mathcal{M}$, the mesh density is $d = (m_\xi m_\eta)^{-1}$. Matrix Λ is a 2×2 diagonal one with eigenvalues $\lambda_1 = \frac{m_\xi}{m_\eta}$ and $\lambda_2 = \frac{m_\eta}{m_\xi}$. It is also useful to identify the mesh sizes $(\delta x, \delta y)$ in Cartesian directions:

$$\delta\mathbf{x}_\mathcal{M} = (\delta x_\mathcal{M}, \delta y_\mathcal{M}) \quad , \quad \delta x_\mathcal{M} = e_\xi^x m_\xi + e_\eta^x m_\eta \quad , \quad \delta y_\mathcal{M} = e_\xi^y m_\xi + e_\eta^y m_\eta\ .$$

In the continuous mesh methods (see for example [11]), the error in linear interpolation was modelled by (we discard the constant):

$$|u_q(\mathbf{x}) - \pi_1^{\mathcal{M}} u_q(\mathbf{x})| \;\approx\; |\frac{\partial^2 u_q}{\partial \tau_q^2}|(\delta\tau_q)^2 + |\frac{\partial^2 u_q}{\partial n_q^2}|(\delta n_q)^2 \;=\; \delta\mathbf{x}_{\mathcal{M}}|H_{u_q}|\delta\mathbf{x}_{\mathcal{M}}$$
$$= \; trace(\mathcal{M}^{-\frac{1}{2}}|H_{u_q}|\mathcal{M}^{-\frac{1}{2}}) \qquad (5)$$

where H_{u_q} is the Hessian of u_q, and orthonormal directions $\tau_q = (\tau_x^q, \tau_y^q)$ and $n_q = (n_x^q, n_y^q)$ are eigrnvectors of this Hessian.

In [12] the authors propose a general statement for an interpolation of arbitrary degree generalizing (5). Here, we follow their proposition by defining the error model for a quadratic reconstruction as follows (for $q = 1, 4$):

$$|u_q(\mathbf{x}) - \pi_2 u_q(\mathbf{x})| \approx \left(|\frac{\partial^3 u_q}{\partial \tau_q^3}|^{\frac{2}{3}} (\delta\tau_q^{\mathcal{M}})^2 + |\frac{\partial^3 u_q}{\partial n_q^3}|^{\frac{2}{3}} (\delta n_q^{\mathcal{M}})^2 \right)^{\frac{3}{2}} .$$

where orthonormal directions $\tau_q = (\tau_x^q, \tau_y^q)$ and $n_q = (n_x^q, n_y^q)$ can be computed from the Silvester decomposition of the cubic term of Taylor formula for u_q. Increments $\delta\tau_q^{\mathcal{M}}$ and $\delta n_q^{\mathcal{M}}$ are local mesh size in these directions:

$$\delta\tau_q^{\mathcal{M}} = \tau_x^q \delta x_{\mathcal{M}} + \tau_y^q \delta y_{\mathcal{M}} \;\; ; \;\; \delta n_q^{\mathcal{M}} = n_x^q \delta x_{\mathcal{M}} + n_y^q \delta y_{\mathcal{M}} \; .$$

Then

$$|\frac{\partial^3 u_q}{\partial \tau_q^3}|^{\frac{2}{3}} (\delta\tau_q)^2 + |\frac{\partial^3 u_q}{\partial n^3}|^{\frac{2}{3}} (\delta n_q)^2 = (S^q \delta\mathbf{x}_{\mathcal{M}}, \delta\mathbf{x}_{\mathcal{M}})$$

with

$$S_{11}^q = (\tau_x^q)^2 |\frac{\partial^3 u_q}{\partial \tau_q^3}|^{\frac{2}{3}} + (n_x^q)^2 |\frac{\partial^3 u_q}{\partial n^3}|^{\frac{2}{3}}$$
$$S_{12}^q = S_{21}^q = (\tau_x^q \tau_y^q) |\frac{\partial^3 u_q}{\partial \tau_q^3}|^{\frac{2}{3}} + (n_x^q n_y^q) |\frac{\partial^3 u_q}{\partial n^3}|^{\frac{2}{3}}$$
$$S_{22}^q = (\tau_y^q)^2 |\frac{\partial^3 u_q}{\partial \tau_q^3}|^{\frac{2}{3}} + (n_y^q)^2 |\frac{\partial^3 u_q}{\partial n^3}|^{\frac{2}{3}}$$

After the *a priori* analysis, we have to minimise the following error:

$$\mathcal{E} \;=\; \sum_{q=1,4} \int K_q(u, u^*) \left(|\frac{\partial^3 u_q}{\partial n_q^2}|^{\frac{2}{3}} (\delta n_q)^2 + |\frac{\partial^3 u_q}{\partial \tau_q^2}|^{\frac{2}{3}} (\delta\tau_q)^2 \right)^{\frac{3}{2}} \; dxdy \; .$$
$$= \; \int (S\delta\mathbf{x}_{\mathcal{M}}, \delta\mathbf{x}_{\mathcal{M}})^{\frac{3}{2}} \; dxdy = \int \left(trace(\mathcal{M}^{-\frac{1}{2}}|S|\mathcal{M}^{-\frac{1}{2}}) \right)^{\frac{3}{2}} \; dxdy.$$

with

$$S_{11} = \sum_{q=1,4} K_q(u,u^*)^{\frac{2}{3}} (\tau_x^q)^2 |\frac{\partial^3 u_q}{\partial \tau_q^3}|^{\frac{2}{3}} + \sum_{q=1,4} K_q(u,u^*)^{\frac{2}{3}} (n_x^q)^2 |\frac{\partial^3 u_q}{\partial n^3}|^{\frac{2}{3}}$$

$$S_{12} = S_{21} = \sum_{q=1,4} K_q(u,u^*)^{\frac{2}{3}} (\tau_x^q \tau_y^q) |\frac{\partial^3 u_q}{\partial \tau_q^3}|^{\frac{2}{3}} + \sum_{q=1,4} K_q(u,u^*)^{\frac{2}{3}} (n_x^q n_y^q) |\frac{\partial^3 u_q}{\partial n^3}|^{\frac{2}{3}}$$

$$S_{22} = \sum_{q=1,4} K_q(u,u^*)^{\frac{2}{3}} (\tau_y^q)^2 |\frac{\partial^3 u_q}{\partial \tau_q^3}|^{\frac{2}{3}} + \sum_{q=1,4} K_q(u,u^*)^{\frac{2}{3}} (n_y^q)^2 |\frac{\partial^3 u_q}{\partial n^3}|^{\frac{2}{3}}. \quad (6)$$

Matrix $S(\mathbf{x})$ is a sum of symmetric positive definite matrices and so is it:

$$S(\mathbf{x}) = \mathcal{R}_S(\mathbf{x}) \Lambda_S(\mathbf{x}) \mathcal{R}_S^t(\mathbf{x})$$

with eigenvectors $\mathbf{n}_S$ and $\boldsymbol{\tau}_S$ and eigenvalues δn_S and $\delta \tau_S$.

Optimal metric. We know identify the optimal metric $\mathcal{M}^{opt} = \mathcal{M}^{opt}(N)$ among those having a prescribed total node number N which minimise the above error. We proceed as for the second-order metric analysis, e.g. [10].

We observe that:

$$\int \left(trace(\mathcal{M}^{-\frac{1}{2}} |S| \mathcal{M}^{-\frac{1}{2}}) \right)^{\frac{3}{2}} \, dxdy = \int \left(trace(d_{\mathcal{M}}^{-1} (\mathcal{R}_{\mathcal{M}} \Lambda_{\mathcal{M}} \mathcal{R}_{\mathcal{M}}^T)^{-\frac{1}{2}} |S| (\mathcal{R}_{\mathcal{M}} \Lambda_{\mathcal{M}} \mathcal{R}_{\mathcal{M}}^T)^{-\frac{1}{2}}) \right)^{\frac{3}{2}} \, dxdy$$

We first prescribe, at each point $\mathbf{x}$ of the computational domain, the adapted metric eigenvectors *i.e.* the representation of the direction of stretching of mesh, $\mathcal{R}_{\mathcal{M}_{opt}} = (\mathbf{e}_\xi^{\mathcal{M}_{opt}}, \mathbf{e}_\eta^{\mathcal{M}_{opt}})$ as aligned with the above error model, that is

$$\mathbf{e}_\xi^{\mathcal{M}_{opt}} = \mathbf{n}_S, \ \mathbf{e}_\eta^{\mathcal{M}_{opt}} = \boldsymbol{\tau}_S.$$

Then, minimising the error at each point $\mathbf{x}$ of the computational domain for a prescribed density $d_{\mathcal{M}}$, we derive that the best ratio of eigenvalues for $\mathcal{M}$, *i.e.* the representation of mesh stretching or anisotropy should be:

$$e_{\mathcal{M}_{opt}} = \frac{(\delta n_S)^{-\frac{1}{2}}}{(\delta \tau_S)^{-\frac{1}{2}}} \ ; \ \Lambda_{\mathcal{M}_{opt}} = diag[e_{\mathcal{M}_{opt}}^{-1}, e_{\mathcal{M}_{opt}}] \ .$$

Inside this restricted set of metrics, it remains to define the optimal metric density. Let us consider the set of metrics with a total number of vertices prescribed to N:

$$\int d \ dxdy = N. \quad (7)$$

We now have to minimise the L^1 norm of the error

$$\begin{aligned} \mathcal{E}(d) &= \int d^{-\frac{3}{2}} \Gamma(S) \ dxdy \\ \Gamma(S) &= \left(trace((\mathcal{R}_{\mathcal{M}_{opt}} \Lambda_{\mathcal{M}_{opt}} \mathcal{R}_{\mathcal{M}_{opt}}^T)^{-\frac{1}{2}} |S| (\mathcal{R}_{\mathcal{M}_{opt}} \Lambda_{\mathcal{M}_{opt}} \mathcal{R}_{\mathcal{M}_{opt}}^T)^{-\frac{1}{2}}) \right)^{\frac{3}{2}} \end{aligned} \quad (8)$$

with respect to d for a given number of nodes N. This means that:

$$\mathcal{E}'(d) \cdot \delta d = 0 \ \ \forall \ \ \delta d \ \ \text{with} \int \delta d \ dxdy = 0$$

which implies that the derivative of integrand in $\mathcal{E}$ is constant:

$$\Gamma(S) d^{-\frac{5}{2}} = constant$$

and produces an optimal density

$$d_{opt} = \frac{N}{C}_{opt} (\Gamma(S))^{\frac{2}{5}}$$

with

$$C_{opt} = \int (\Gamma(S))^{\frac{2}{5}} \ dxdy.$$

This completes the definition of the optimal metric:

$$\mathcal{M}_{opt} = d_{opt} \mathcal{R}^t_{opt} \begin{pmatrix} e^{-1}_{opt} & 0 \\ 0 & e_{opt} \end{pmatrix} \mathcal{R}_{opt}.$$

4. Conclusion

5. Acknowledgements

This work has been supported by French National Research Agency (ANR) through COSINUS program (project ECINADS n^o ANR-09-COSI-003). HPC resources from GENCI-[CINES] (Grant 2010-x2010026386 and 2010-c2009025067) are also gratefully acknowledged.

References

[1] A. Dervieux A. Carabias, O. Allain. Dissipation and dispersion control of a quadratic-reconstruction advection scheme. In *In European Workshop on High Order Nonlinear Numerical Methods for Evolutionary PDEs: Theory and Applications*, Trento, Italy, april 11-15 2011.

[2] T.J. Barth. Recent developements of high-order k-exact reconstruction on unstructured meshes. In *31st AIAA Aerospace Science Meeting*, AIAA-93-0668, Reno, NV, USA, 1993.

[3] T.J. Barth and M.G. Larson. A-posteriori error estimation for higher order godunov finite volume methods on unstructured meshes. In R. Herbin and D. Kröner, editors, *Finite Volumes for Complex Applications III*, pages 41–63. 41 63, 2002.

[4] A. Belme, F. Alauzet, and A. Dervieux. A priori anisotropic goal-oriented estimate and mesh adaptation for viscous compressible flow. *Preprint*, 2012.

[5] A. Belme, A. Dervieux, and F. Alauzet. A fully anisotropic goal-oriented mesh adaptation for unsteady flows. In *Proceedings of the V ECCOMAS CFD Conf.*, 2010.

[6] A. Belme, A. Dervieux, and F. Alauzet. Time accurate anisotropic goal-oriented mesh adaptation for unsteady flows. *J. Comp. Phys.*, 2012. http://www-sop.inria.fr/members/Alain.Dervieux/Adj-Insta-2011_10.pdf.

[7] Weiming Cao. An interpolation error estimate on anisotropic meshes in r^n and optimal metrics for mesh refinement. *SIAM J. Numer. Anal.*, 45(6):2368 2391, 2007.

[8] I. Abalakin B. Koobus H. Ouvrard, T. Kozubskaya and A. Dervieux. Advective vertex-centered recon- struction scheme on unstructured meshes. RR-7033, INRIA, 2009.

[9] L. Ivan and C. P. T. Groth.

[10] A. Loseille, A. Dervieux, P.J. Frey, and F. Alauzet. Achievement of global second-order mesh convergence for discontinuous flows with adapted unstructured meshes. In *37th AIAA Fluid Dynamics Conference and Exhibit*, AIAA-2007-4186, Miami, FL, USA, Jun 2007.

[11] A. Loseille and journal = SIAM in Numerical Analysis volume = 49 number = 1 year = 2011 F. Alauzet, title = Continuous mesh framework, Part I: well-posed continuous interpolation error.

[12] E. Mbinky, F. Alauzet, and A. Loseille. High order interpolation ofr mes adaptation. In *Proceedings of ECCOMAS CFD*, Vienna, Austria, 2012.